

## FLUX-STABILITY ANALYSIS FOR THE COMPARISON STARS FOR SOME QUASARS IMPORTANT TO ICRF - GAIA CRF LINK

MILJANA D. JOVANOVIĆ, GORAN DAMLJANOVIĆ  
and OLIVER VINCE

*Astronomical Observatory, Volgina 7, 11060 Belgrade, Serbia*  
E-mail: miljana@aob.rs, gdamljanovic@aob.rs, ovince@aob.rs

**Abstract.** The Gaia astrometric mission will provide a catalog of about 600 000 quasars and billion stars. Some of these quasars could be the basis of a new optical reference frame. It is necessary to observe a set of common objects (mostly quasars) at both optical and radio wavelengths to link the future Gaia Celestial Reference Frame - Gaia CRF (at optical wavelength) with the ICRF (based on the VLBI observations of sources at radio wavelengths). To establish this link only 10% of the ICRF sources (about 70 ones) are suitable, and because of that this number has been increased by 47 objects (out of the ICRF list) with high astrometric quality. Our observations of 47 candidate sources have been carried out by using three telescopes: two of them with  $D=0.6\text{m}$  and  $D=1.4\text{m}$  are located at the Astronomical Station Vidojevica (of the Astronomical Observatory of Belgrade) and the third one with  $D=2\text{m}$  at the Rozhen NAO BAS (Bulgaria). In this paper we present light curves of a few objects, together with their comparison stars for the period from mid-2016 until now. Also, the results of the flux-stability analysis for the comparison stars are presented here.

### 1. INTRODUCTION

The European Space Agency mission GAIA (Global Astrometric Interferometer for Astrophysics) was launched in December 2013. The first Gaia data release (Gaia DR1) was made publicly available in September 2016 (Lindegren et al. 2016), and the second one (Gaia DR2) in April 2018 (Gaia Collaboration et al. 2018). The second Gaia release provides complete 5 astrometric parameters (positions, parallaxes, and proper motions) for more than 1.3 billion sources. Plus, the approximate positions for an additional near 0.4 billion mostly faint sources. The reference epoch is J2015.5 (Lindegren et al. 2018).

One of the most important results of the Gaia mission will be a new highly-accurate optical Gaia Celestial Reference Frame (Gaia CRF). That new Gaia CRF will be at the same level of accuracy as the International Celestial Reference Frame (ICRF) that is established in the radio domain by VLBI observations of selected sources (mostly quasars - QSOs). The axes of Gaia CRF will be fixed with respect to distant extragalactic objects. Because of continuity the orientation of the Gaia CRF axes should coincide with the ICRF.

The basic idea to tie the Gaia catalog to the ICRF, is using Gaia observations in optical domain of compact extragalactic ICRF objects with accurate radio positions. Only about 70 sources from ICRF are suitable to establish this link, and because of that this number has increased by 47 sources (out of the ICRF list) with high astrometric quality (Bourda *et al.* 2011).

There are several papers about some investigation of the flux variability (one of the properties of QSOs) and photocentre motion of QSOs. Taris *et al.* (2011, 2016), Popovic *et al.* (2012) have reported numerical values for the photocentre jitter between some tens of  $\mu\text{as}$  to some  $\text{mas}$ . The QSOs with more stable flux should be the base for the link between Gaia CRF and ICRF. Thus, it is necessary to monitor flux stability of QSOs over a longer period of time. In this way, we could determine QSOs with a more stable flux and to eliminate objects with variable photocentre.

## 2. OBSERVATIONS AND RESULTS

We started with observations of mentioned 47 candidate sources since July 2016 using two telescopes at the Astronomical Station Vidojevica - ASV (of the Astronomical Observatory of Belgrade), and 2 m telescope at the Rozhen NAO BAS (Bulgaria) in accordance with the joint Serbian - Bulgarian research project.

**Table 1:** The main information about telescopes and used CCD cameras.

Site ASV	CCD camera Apogee Alta E47
Telescope Cassegrain	pixel array 1024x1024, scale 0.''45
D/F = 60/600 cm	pixel size 13x13 $\mu\text{m}$ and $FoV = 7.'6 \times 7.'6$
Site Rozhen	CCD camera Andor iKon-L
Telescope Ritchey-Chrétien	pixel array 2048x2048, scale 0.''17
D/F = 200/1577 cm	pixel size 13.5x13.5 $\mu\text{m}$ and $FoV = 6' \times 6'$

The characteristics of the 60 cm ASV telescope (with longitude  $\lambda = 21.5^\circ\text{E}$ , latitude  $\varphi = 43.1^\circ\text{N}$ , altitude  $h=1140$  m) and 2 m Rozhen telescope ( $\lambda=24.7^\circ\text{E}$ ,  $\varphi=41.7^\circ\text{N}$ ,  $h=1730\text{m}$ ) with CCD cameras are presented in Table 1. The FoV is field of view. For the other instruments, see in papers (Damljanović *et al.* 2014, Jovanović *et al.* 2018). The Johnson-Cousins BVRI filters were available. The standard bias, dark and flat-fielded corrections (plus hot/dead pixels, cosmic rays, etc.) for CCD images are done by using IRAF scripting language.

FLUX-STABILITY ANALYSIS FOR THE COMPARISON STARS

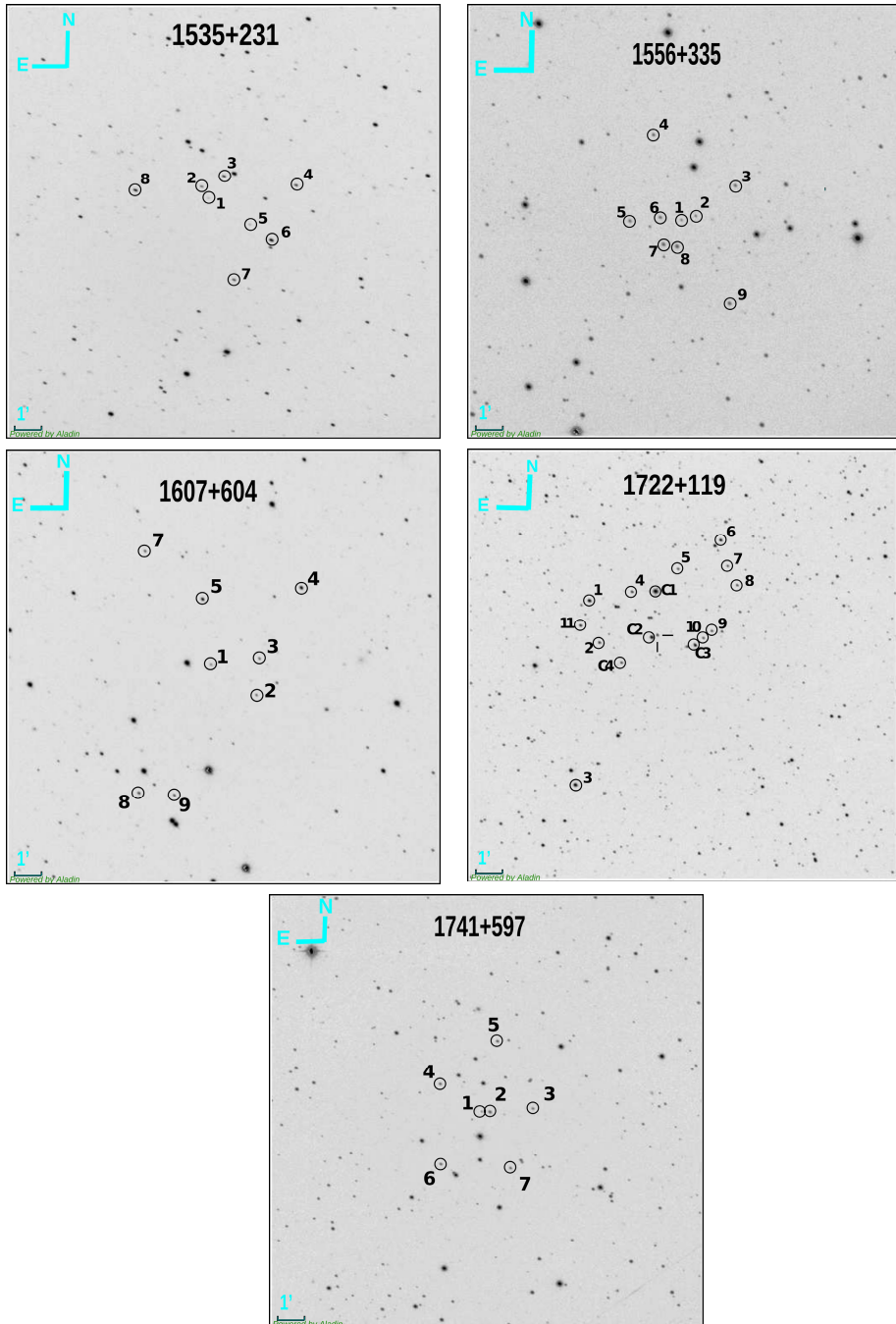


**Figure 1:** Charts of the fields of objects 1535+231, 1556+335, 1607+604, 1722+119, 1741+597.

Charts of the fields of objects were created using CCD images taken with ASV 60cm and CCD camera Apogee Alta U42 (Fig 1.). In Fig 1. the designation 1 refers to the specific objects from the figure caption and the other numbers refer to comparison stars around the object with exception of 1722+119 where the object is indicated by cross and the other objects are comparison stars.

**1722+119.** This object is a variable BL Lacertae (BL Lac) with redshift  $z=0.018$ . We chose comparison stars with their V and R magnitudes from Doroshenko et al. (2014). They were selected so that some stars are brighter than and some of them are fainter than object. This object has the highest number of comparison stars; we chose 8, out of the 15 stars given in Doroshenko et al. (2014). Comparison stars C2, C3 and 1 are very bright, and were not used for photometry on CCD images where they were saturated.

This object was observed during the period of 776 days, and during that period the V and R magnitudes show some variability (maybe periodicity) in both filters. The average magnitudes in that period are 15.230 (standard deviation,  $\sigma=0.130$ ) in V filter and 14.722 ( $\sigma=0.180$ ) in R filter. The obtained extremal magnitudes (maximum and minimum values) are: 14.904 and 15.438 in V filter, 14.366 and 14.996 in R filter, respectively. The standard deviation range of comparison stars is from 0.010 (comparison star C2) to 0.045 (star 5) in V filter, and 0.017 (C4) to 0.033 (10) in R filter.

**1535+231, 1556+335, 1607+604, and 1741+597.** For these objects we chose comparison stars from the SDSS DR14 catalog (<https://www.sdss.org/dr14/>, Abolfathi et al. 2018). The PSF ugriz-magnitudes were transformed into BVRI using suitable transformations (Chonis and Gaskel 2008).

Comparison stars that we selected for 1535+231 and 1741+597 are much brighter than the objects themselves, but we had to choose stars that better satisfy some criteria (see below). It is not the case with 1556+335 and 1607+604; some of the stars in their vicinity are similar in brightness to these objects, but all stars satisfy criteria (see below) very well. For objects 1535+231 (from 28<sup>th</sup> April 2017 to 23<sup>th</sup> April 2018) and 1607+604 (from 4<sup>th</sup> August 2016 to 15<sup>th</sup> September 2017), changing CCD cameras on the ASV telescopes caused a change in size of the FoV and, consequently, some of comparison stars could not be able to observe.

Quasar 1535+231, with redshift  $z=0.46252$ , during our observational period of 772 days, has average magnitudes of 18.315 ( $\sigma=0.166$ ) in V and 18.047 ( $\sigma=0.182$ ) in R. The standard deviation of comparison stars is in the range from 0.010 (comparison star 8 in V filter) to 0.039 (star 2 in R filter). The obtained extremal magnitudes of object during that period are: 18.067 and 18.654 in V filter, 17.803 and 18.450 in R filter, respectively. The brightness of object has decreased for about 0.6 magnitude in both filters.

Quasar 1556+335 (redshift  $z=1.65348$ ) was observed during 776 days. Photometrically, that object is the most stable one, with the average magnitudes of 17.476 ( $\sigma=0.040$ ) in V filter and 16.977 ( $\sigma=0.036$ ) in R filter. The standard deviation of its comparison stars is in the range from 0.006 (star 7) to 0.033 (star 2) in R filter.

Object 1607+604 is BL Lac with redshift  $z=0.178$ . This object was also observed during 776 days. Average magnitudes for this period were: 17.468 with  $\sigma=0.087$  in V filter, and 17.039 with  $\sigma=0.079$  in R filter. The lowest standard deviation  $\sigma=0.019$  has comparison star 4 in R filter, and the highest one  $\sigma=0.050$  has star 2 in V filter.

Object 1741+597 is also BL Lac with redshift  $z=0.4$ . During 775 days, this object had average magnitudes 18.053 ( $\sigma=0.206$ ) in V filter and 17.634 ( $\sigma=0.252$ ) in R filter; these standard deviations are bigger than others. The magnitude range is from 18.430 to 17.689 in V, and 18.116 to 17.174 in R. It is interesting that the brightness of this object has increased for almost 1 magnitude in both filters. The standard deviation range of comparison stars is from 0.014 (star 4) to 0.036 (star 5) in V filter.

Because of detected changes in magnitudes, objects 1535+231, 1722+119 and 1741+597 are selected to investigate possibility of their intranight changes.

The redshifts were taken from the NASA/IPAC Extragalactic Database - NED (<https://ned.ipac.caltech.edu/>), and objects type from SIMBAD Astronomical Database.

From SDSS catalog we chose stars following several criteria: not too far from the objects, not too bright or faint stars (with  $g$ ,  $r$  and  $i$  magnitudes outside the range 14.5 – 19.5) or not very blue or red (outside the ranges  $0.08 < r-i < 0.5$  and  $0.2 < g-r < 1.4$ ), not variable stars, etc. The PSF ugriz magnitudes of the comparison stars were transformed into the Johnson-Cousins BVRI (Chonis and Gaskel 2008) using equations:

$$V = g - (0.587 \pm 0.022)(g - r) - (0.011 \pm 0.013)$$

$$R = r - (0.272 \pm 0.092)(r - i) - (0.159 \pm 0.022).$$

Obtained V and R magnitudes (Table 2.) were our input values for the Analyze tool Photometry in MaxIm DL software. With that tool, which is used for differential photometry, the magnitudes of selected objects and their comparison stars were calculated for each epoch of observation. These output values of the magnitudes of comparison stars for the period of about 2 years were used for flux-stability analysis; the average values of magnitudes are in Table 3. The flux-stability analysis was examined with  $3\text{-}\sigma$  criteria. In accordance with that criteria, we did not detect variability in V and R of comparison stars. In line with standard deviations of stars, the input and output values of suitable magnitudes of stars are close to each other (see Table 2. and 3.). In Fig. 2, the light curves of objects and their comparison stars (output V and R magnitudes) are presented. As we can see, the stars are stable, but some objects show changeable flux during observed period. There are two gaps during the observations due to bad weather conditions, and lack of data for V filter due to technical problems that existed in the period from 7<sup>th</sup> July to 31<sup>th</sup> October 2016.

**Table 2:** Coordinates and magnitudes (V and R) with standard errors of comparison stars for objects 1535+231, 1556+335, 1607+604, 1722+119, 1741+597.

Object	No.	$\alpha_{J2000.0} [^{\circ}]$	$\delta_{J2000.0} [^{\circ}]$	$V \pm \sigma_V [\text{mag}]$	$R \pm \sigma_R [\text{mag}]$
1535+231	2	234.314909	23.01831	17.200 $\pm$ 0.068	16.658 $\pm$ 0.071
	3	234.300042	23.02486	15.983 $\pm$ 0.065	15.633 $\pm$ 0.060
	4	234.251776	23.01917	16.232 $\pm$ 0.053	15.867 $\pm$ 0.056
	7	234.293122	22.96096	16.470 $\pm$ 0.058	15.973 $\pm$ 0.067
	8	234.359173	23.01592	15.860 $\pm$ 0.074	15.149 $\pm$ 0.086
1556+335	2	239.719504	33.39110	17.336 $\pm$ 0.066	16.850 $\pm$ 0.073
	3	239.690349	33.40959	16.381 $\pm$ 0.057	16.095 $\pm$ 0.056
	5	239.767982	33.38778	16.271 $\pm$ 0.063	15.916 $\pm$ 0.060
	6	239.745615	33.39003	16.198 $\pm$ 0.064	15.825 $\pm$ 0.061
	7	239.743174	33.37370	15.552 $\pm$ 0.063	15.188 $\pm$ 0.060
	8	239.733984	33.37219	15.743 $\pm$ 0.082	14.897 $\pm$ 0.104
1607+604	2	242.028820	60.28951	17.068 $\pm$ 0.059	16.619 $\pm$ 0.058
	3	242.025260	60.31162	16.864 $\pm$ 0.055	16.423 $\pm$ 0.061
	4	241.973520	60.35552	15.195 $\pm$ 0.054	14.781 $\pm$ 0.059
	5	242.096377	60.34816	15.630 $\pm$ 0.064	14.965 $\pm$ 0.078
	7	242.168538	60.37746	16.856 $\pm$ 0.053	16.467 $\pm$ 0.060
1722+119	c2	261.271667	11.86997	13.173 $\pm$ 0.005	12.570 $\pm$ 0.006
	c3	261.243750	11.86636	14.078 $\pm$ 0.012	13.600 $\pm$ 0.008
	1	261.312083	11.89125	13.445 $\pm$ 0.009	12.848 $\pm$ 0.010
	2	261.304583	11.86519	14.823 $\pm$ 0.008	14.691 $\pm$ 0.012
	5	261.256667	11.91311	15.873 $\pm$ 0.010	15.385 $\pm$ 0.016
	9	261.233333	11.87083	15.809 $\pm$ 0.008	15.332 $\pm$ 0.014
	10	261.238750	11.87083	16.142 $\pm$ 0.011	15.699 $\pm$ 0.019
c4	261.289583	11.85344	15.665 $\pm$ 0.009	15.164 $\pm$ 0.013	
1741+597	2	265.623286	59.75176	15.565 $\pm$ 0.062	15.204 $\pm$ 0.063
	3	265.570814	59.75387	16.673 $\pm$ 0.063	16.314 $\pm$ 0.062
	4	265.684115	59.76861	16.376 $\pm$ 0.073	15.795 $\pm$ 0.073
	5	265.614574	59.79547	16.154 $\pm$ 0.067	15.704 $\pm$ 0.064
	6	265.682817	59.71901	16.126 $\pm$ 0.082	15.684 $\pm$ 0.085
	7	265.597661	59.71686	16.633 $\pm$ 0.085	16.124 $\pm$ 0.091

**Table 3:** Average magnitudes (V and R) with standard errors of comparison stars for objects 1535+231, 1556+335, 1607+604, 1722+119, 1741+597; period July 2016 - August 2018.

Object No.	1535+231		No.	1607+604	
	V $\pm\sigma_V$ [mag]	R $\pm\sigma_R$ [mag]		V $\pm\sigma_V$ [mag]	R $\pm\sigma_R$ [mag]
2	17.217 $\pm$ 0.025	16.699 $\pm$ 0.039	2	17.068 $\pm$ 0.050	16.635 $\pm$ 0.036
3	16.009 $\pm$ 0.018	15.661 $\pm$ 0.034	3	16.886 $\pm$ 0.033	16.477 $\pm$ 0.029
4	16.237 $\pm$ 0.017	15.847 $\pm$ 0.017	4	15.184 $\pm$ 0.032	14.760 $\pm$ 0.019
7	16.447 $\pm$ 0.023	15.955 $\pm$ 0.023	5	15.618 $\pm$ 0.021	14.970 $\pm$ 0.020
8	15.836 $\pm$ 0.010	15.138 $\pm$ 0.022	7	16.848 $\pm$ 0.027	16.409 $\pm$ 0.027
	1556+335			1741+597	
2	17.336 $\pm$ 0.022	16.857 $\pm$ 0.033	2	15.591 $\pm$ 0.016	15.251 $\pm$ 0.029
3	16.364 $\pm$ 0.023	16.032 $\pm$ 0.022	3	16.648 $\pm$ 0.024	16.292 $\pm$ 0.016
5	16.277 $\pm$ 0.017	15.892 $\pm$ 0.022	4	16.383 $\pm$ 0.014	15.799 $\pm$ 0.017
6	16.212 $\pm$ 0.014	15.834 $\pm$ 0.012	5	16.161 $\pm$ 0.036	15.711 $\pm$ 0.018
7	15.556 $\pm$ 0.014	15.183 $\pm$ 0.006	6	16.110 $\pm$ 0.022	15.658 $\pm$ 0.023
8	15.736 $\pm$ 0.029	14.926 $\pm$ 0.008	7	16.599 $\pm$ 0.022	16.072 $\pm$ 0.023
	1722+119				
C2	13.174 $\pm$ 0.010	12.602 $\pm$ 0.018	5	15.866 $\pm$ 0.045	15.351 $\pm$ 0.030
C3	14.080 $\pm$ 0.015	13.603 $\pm$ 0.021	9	15.802 $\pm$ 0.012	15.317 $\pm$ 0.032
1	13.436 $\pm$ 0.020	12.822 $\pm$ 0.028	10	16.132 $\pm$ 0.025	15.689 $\pm$ 0.033
2	14.832 $\pm$ 0.018	14.656 $\pm$ 0.018	C4	15.654 $\pm$ 0.021	15.146 $\pm$ 0.017

## 5. CONCLUSIONS

In Fig 2. are shown the light curves of objects 1535+231, 1556+335, 1607+604, 1722+119 and 1741+597 with light curves of their comparison stars (output values). For the period of about 2 years, the 3- $\sigma$  criteria were applied for all listed comparison stars. Some of the objects show changeable flux during observed period, and stars are stable (in line with mentioned criteria). In the measurements of flux of comparison stars any systematic variation was not detected. In line with values of standard deviations, the suitable input and output magnitudes of stars are close to each other. Our next step is to examine magnitude stability of the objects using statistical methods (as F-test,  $\chi^2$  one) and to investigate their quasiperiodicities. Also, the presented sets of comparison stars could be used for future investigations of mentioned objects.

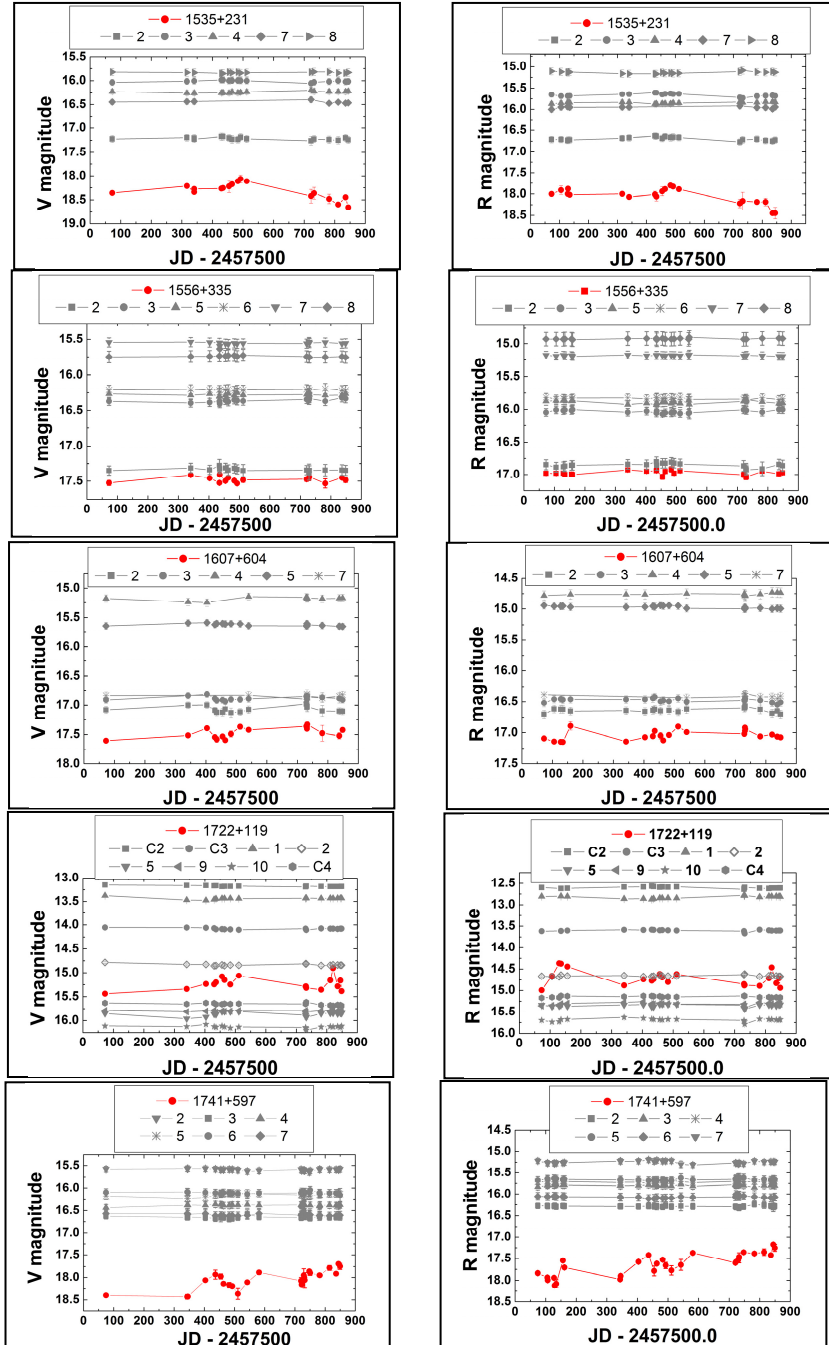


**Figure 2:** The light curves of V and R magnitudes of the objects and their comparison stars, from July 2016 until August 2018.

### Acknowledgment

We gratefully acknowledge the observing grant support from the Institute of Astronomy and NAO Rozhen, BAS, via bilateral joint research project “Study of ICRF radio-sources and fast variable astronomical objects” for the period 2017-2019. This work is part of the projects 176011 “Dynamics and kinematics of celestial bodies and systems”, 176004 “Stellar physics” and 17021 “Visible and invisible matter in nearby galaxies: theory and observations” supported by the Ministry of Education, Science and Technological Development of the R. of Serbia.

### References

- Abolfathi, B., Aguado, D. S., Aguilar, G., et al.: 2018, *ApJS*, **235**, 42.  
 Bourda, G., Collioud, A., Charlot, P., Porcas, R., Garrington, S.: 2011, *A&A*, **526**, A102.  
 Chonis, T. S., Gaskell, C. M.: 2008, *The Astronomical Journal*, **135**, 264.  
 Damljanić, G., Vince, O., Boeva, S.: 2014, *Serb. Astron. J.*, **188**, 85-93.  
 Doroshenko, V. T., Efimov, Yu. S., Borman, G. A., Pulatova, N. G.: 2014, *Astrophysics*, **57**, 2.  
 Gaia Collaboration, Brown, A. G. A., Vallenari, A., Prusti, T., et al.: 2018, *A&A*, **616**, A1.  
 Jovanović, M. D., Damljanić, G., Vince, O.: 2018, *Publ. Astron. Obs. Belgrade*, **98**, 293 – 296.  
 Lindegren, L., Lammers, U., Bastian, U., et al.: 2016, *A&A*, **595**, A4.  
 Lindegren, L., Hernández, J., Bombrun, A., et al.: 2018, *A&A*, **616**, A2.  
 Popović, L. Č., Jovanović, P., Stalevski, M., et al.: 2012, *A&A*, **538**, A107.  
 Taris, F., Souchay, J., Andrei, A. H., et al.: 2011, *A&A*, **526**, A25.  
 Taris, F., Andrei, A., Roland, J., et al.: 2016, *A&A*, **587**, A112.